Using Interim Recommitment to Reduce the Operational-Cost Impact of Wind Uncertainty

Mahan A. Mansouri, *Student Member, IEEE,* and Ramteen Sioshansi, *Fellow, IEEE*

***Abstract*—Using wind-availability forecasts in day-ahead unit commitment can require expensive real-time operational adjustments. We examine the benefit of conducting interim recommitment between day-ahead unit commitment and real-time dispatch. Using a simple stylized example and a case study that is based on ISO New England, we compare system-operation costs with and without interim recommitment. We find an important tradeoff—later recommitment provides better wind-availability forecasts, but the system has less flexibility due to operating constraints. Of the time windows that we examine, hour-20 recommitment provides the greatest operational-cost reduction.**

***Index Terms*—Power-system operations, power-system economics, unit commitment, economic dispatch, wind generation**

I. Introduction

WIND generation increases supply variability and uncertainty, which requires changing power-system operations to ensure real-time balance between energy supply and demand [1]. These adjustments give rise to what we term 'operational wind-integration costs'. The literature assesses and surveys the impacts of integrating wind generation into power systems [2]–[5]. Western Wind and Solar Integration Study (WWSIS) [6]–[8] examines integrating up to 35% (on an energy basis) wind and solar generation into Western Interconnection. WWSIS examines high renewable-energy penetrations, their impacts on the fossil-fueled generating fleet, and dynamic power-system performance.

The literature studies means of mitigating operational wind-integration costs. One approach uses synergistic technologies, *e.g.*, demand response [9]–[12], energy storage [13]–[17], or flexible electric-vehicle charging [18]–[22]. These technologies increase demand-side flexibility, reducing the need for supply-side adjustments to maintain energy balance. Financial instruments [23], [24] are another option to reduce operational wind-integration costs.

Alternatively, operational wind-integration costs can be reduced by modifying power-system operations. Such adjustment can be done using a stochastic, robust, or distributionally robust approach to modeling unit commitment [25]–[30]. Such approaches account explicitly for uncertain real-time wind availability in deciding unit commitment and dispatch. Another approach is to conduct rolling-horizon optimization, which allows updated wind-availability information to be incorporated into operational planning [31]. Tuohy *et al*. [32] combine these two concepts, by incorporating rolling-horizon decision-making into a stochastic-optimization framework.

Operational planning with explicit uncertainty characterization presents challenges. For one, market operators have a short time window following gate closure to provide day-ahead operating schedules and prices to market participants. The capabilities of optimization software and computational hardware are considerably greater than those available at the advent of stochastic unit commitment [26], [28], [29], [33]. Nevertheless, the complexities of market models may make market operators wary for the foreseeable future of adopting such models. Another important challenge relates to price formation. Stochastic unit-commitment models produce scenario-dependent dispatch schedules and prices, which complicate market settlement [34]. Of importance to a market operator, stochastic prices are revenue-adequate in expectation only. Thus, depending upon realized real-time wind availability, the market operator may suffer a revenue deficit. Stochastic prices also may raise incentive-compatibility issues.

As such, operational models with explicit uncertainty characterization see limited use today by *any* market operator. Instead, most market operators rely on deterministic models [35], [36].[1] Given these realities, the aim of our work is to explore the benefits of introducing recommitment between day-ahead and real-time market operations. As such, our work expands upon the concept that Tuohy *et al*. [31] study. However, we extend the work of Tuohy *et al*. in a number of key ways. First, we model and explore the tradeoff between generator flexibility and forecast quality. Conducting recommitment closer to the trading day (*e.g.*, during hour 23 as opposed to hour 18) provides better wind-availability forecasts. However, operating constraints may limit the ability of some generators to adjust their operation if the recommitment is conducted closer to real time. We capture such intertemporal dynamics by developing a detailed operational model that is solved in a manner that mimics the time sequence of real-world market operations. A second distinction of our work is that we apply it to a comprehensive case study that is based on ISO New England, over a one-year study horizon. Tuohy *et al*. [31] examine system operations over a three-week period. Thus, our work examines the benefits of recommitment, considering diurnal and seasonal load and wind-availability patterns.

Our case study shows reduced operational wind-integration costs with recommitment compared to having only day-ahead

Manuscript received: 17 August, 2021; accepted: xx Xxxx, 2022. Date of CrossCheck: xx Xxxx, 2022. Date of online publication: xx Xxxx, 2022. This work is supported by National Science Foundation grant 1808169.

M. A. Mansouri (corresponding author) is with Department of Integrated Systems Engineering, The Ohio State University, Columbus, OH 43210, USA (e-mail: mansouri.2@buckeyemail.osu.edu).

R. Sioshansi is with Department of Integrated Systems Engineering, Department of Electrical and Computer Engineering, and Center for Automotive Research, The Ohio State University, Columbus, OH 43210, USA (e-mail: sioshansi.1@osu.edu).

[1] http://www.caiso.com/Documents/1_CaliforniaISO_MarketOverview.pdf

and real-time market operations. Among the time windows that we examine, hour-20 recommitment minimizes operational wind-integration costs, suggesting that hour 20 balances wind-forecast quality with operational flexibility of the system. However, this result is specific to our case study.

Our work makes two contributions to the extant literature. First, we propose a comprehensive approach to modeling market operations that can be applied to studying the benefits of introducing recommitment to reduce operational wind-integration costs. The models that we use are not novel. The novelty of our work is in implementing these models in a realistic manner that mimics real-world power-system operations. As such, our approach can be applied to other systems with different resource mixes and load and weather patterns. Second, our case study demonstrates the tradeoff between forecast quality and generator flexibility. If market operators intend to introduce recommitment, our modeling approach and metrics could be employed to optimize the timing of the processes.

The remainder of this paper is organized as follows. Section II provides our model formulation. Section III details the simulation approach. Section IV provides the data that underlie and results of an illustrative example. Section V summarizes data for our comprehensive case study. Sections VI and VII provide case-study results and conclude, respectively.

II. Unit-Commitment Model

A. Model Nomenclature

1) Sets and Indices: We model system operations at hourly time steps over the ordered set, $T = \{t_{\text{st}}, t_{\text{st}}+1, \ldots, t_{\text{en}}\}$, of hours in the optimization horizon and define t as the time index. b is the index for buses, which are in the set, B. We define sets, I and Ω, of non-wind and wind generators, respectively, and let i be the generator index. We define $I(b)$ as the set of generators that are located at bus b. We define a set, L, of transmission lines and let l be the transmission-line index. Non-wind generators are modeled as having an ordered set, K, of start-up types, which correspond to how long the unit has been offline when it is started, and we let k denote the start-up-type index.

2) Parameters and Functions: Non-wind generators are assumed to have a three-part cost structure. c_i^N is the fixed no-load cost (\$/h) of having non-wind generator i online. $c_i^V(\cdot)$ gives the output-dependent cost function (\$) of non-wind generator i. $\bar{c}_{i,k}^S$ is the cost (\$/start-up) of non-wind generator i incurring a type-k start-up. For all $k \in K, k \neq |K|$, non-wind generator i incurs a type-k start-up if it has been offline between $\bar{c}_{i,k}^T$ and $\bar{c}_{i,k+1}^T - 1$ hours when it is started up. If non-wind generator i has been offline $\bar{c}_{i,|K|}^T$ or more hours when it is started up, then it incurs a type-$|K|$ start-up. Wind generators are costless to operate.

Non-wind generator i must produce between K_i^- MW and K_i^+ MW while it is online and must produce 0 MW while it is offline. In addition, generator i's output can decrease by at most R_i^- MW and increase by at most R_i^+ MW between one hour and the next. Non-wind generator can provide up to $\bar{\rho}_i^N$ MW and $\bar{\rho}_i^S$ MW of non-spinning and spinning reserves, respectively. In addition, non-wind generator must be offline a minimum of τ_i^- hours after it is shutdown and must be online a minimum of τ_i^+ hours after it is started-up. Wind generator i has a Z_i-MW nameplate capacity and $\zeta_{t,i}$ is its p.u. hour-t availability factor.

There is $D_{t,b}$ MW of load at bus b during hour t. η is the p.u. load-based reserve requirement and η^S is the p.u. spinning-reserve requirement. Transmission line l has an F_l-MW flow limit and $\Gamma_{l,b}$ is the p.u. bus-b/transmission-line-l shift factor. M is an arbitrarily large constant.

3) Variables: We represent the status of non-wind generators using four sets of binary variables. $u_{t,i}$ equals 1 if non-wind generator i is online during hour t and equals 0 otherwise. $s_{t,i}$ equals 1 if non-wind generator i is started-up during hour t and equals 0 otherwise. In addition, $r_{t,i,k}$ equals 1 if non-wind generator i incurs a type-k start-up during hour t and equals 0 otherwise. $h_{t,i}$ equals 1 if non-wind generator i is shutdown at time t and equals 0 otherwise. Two additional sets of binary variables capture the operation of non-wind generators *vis-à-vis* the provision of operating reserves. $\gamma_{t,i}$ equals 1 if non-wind generator i is the largest hour-t contingency (which prevents it contributing towards the hour-t reserve requirement) and equals 0 otherwise. $\mu_{t,i}$ equals 0 if non-wind generator i cannot provide hour-t non-spinning reserves due to a minimum-down-time constraint and equals 1 otherwise.

$q_{t,i}$ gives generator i's hour-t power output (MW) and $\rho_{t,i}^N$ and $\rho_{t,i}^S$ represent hour-t non-spinning and spinning reserves (MW), respectively, that are provided by non-wind generator i. Wind generators are disallowed from providing operating reserves. $\phi_{t,i}$ gives the number of hours that non-wind generator i is offline as of the beginning of hour t and $m_{t,i}$ measures the number of hours beyond $\bar{c}_{i,|K|}^T$ that non-wind generator i is offline as of the beginning of hour t. $c_{t,i}^S$ represents the actual start-up cost (\$) that is incurred by non-wind generator i during hour t.

Each hour's total reserve requirement is the sum of a p.u. proportion of the hourly system-wide load and the system's largest contingency during the hour. These reserve requirements are based on current practice of California Independent System Operator, which manages a system with relative high renewable-energy penetrations. η_t^v represents the hour-t contingency-based reserve requirement (MW). $\tilde{\rho}_t^N$ and $\tilde{\rho}_t^S$ represent hour-t non-spinning and spinning reserves (MW) that are curtailed. $\tilde{d}_{t,b}$ measures curtailed hour-t load at bus b (MW). $w_{t,b}$ measures hour-t net power (MW) that is withdrawn from the transmission network into bus b.

B. Model Formulation

We model system operations using the mixed-integer linear optimization problem:

$$\min \sum_{t\in T}\left\{\sum_{i\in I}\left[c_{t,i}^S + c_i^N u_{t,i} + c_i^V(q_{t,i})\right] + M\cdot\left(\sum_{b\in B}\tilde{d}_{t,b} + \tilde{\rho}_t^S + \tilde{\rho}_t^N\right)\right\} \quad (1)$$

$$\text{s.t.} \quad \sum_{i\in I(b)} q_{t,i} + w_{t,b} = D_{t,b} - \tilde{d}_{t,b}; \forall t \in T, b \in B \tag{2}$$

$$\sum_{b\in B} w_{t,b} = 0; \forall t \in T \tag{3}$$

$$-F_l \leq \sum_{b\in B} \Gamma_{l,b} w_{t,b} \leq F_l; \forall t \in T, l \in L \tag{4}$$

$$\eta_t^v \geq q_{t,i}; \forall t \in T, i \in I \tag{5}$$

$$\eta_t^v \leq q_{t,i} + (1-\gamma_{t,i})K_i^+; \forall t \in T, i \in I \tag{6}$$

$$\sum_{i\in I} \gamma_{t,i} = 1; \forall t \in T \tag{7}$$

$$\tilde{\rho}_t^S + \tilde{\rho}_t^N + \sum_{i\in I} \left(\rho_{t,i}^S + \rho_{t,i}^N\right) \geq \eta \sum_{b\in B} D_{t,b} + \eta_t^v; \forall t \in T \tag{8}$$

$$\tilde{\rho}_t^S + \sum_{i\in I} \rho_{t,i}^S \geq \eta^S \cdot \left(\eta \sum_{b\in B} D_{t,b} + \eta_t^v\right); \forall t \in T \tag{9}$$

$$0 \leq q_{t,i} \leq \zeta_{t,i} Z_i; \forall t \in T, i \in \Omega \tag{10}$$

$$K_i^- u_{t,i} \leq q_{t,i}; \forall t \in T, i \in I \tag{11}$$

$$q_{t,i} + \rho_{t,i}^S \leq K_i^+ u_{t,i}; \forall t \in T, i \in I \tag{12}$$

$$q_{t,i} + \rho_{t,i}^S + \rho_{t,i}^N \leq K_i^+; \forall t \in T, i \in I \tag{13}$$

$$R_i^- \leq q_{t,i} - q_{t-1,i}; \forall t \in T, i \in I \tag{14}$$

$$q_{t,i} - q_{t-1,i} + \rho_{t,i}^S + \rho_{t,i}^N \leq R_i^+; \forall t \in T, i \in I \tag{15}$$

$$0 \leq \rho_{t,i}^S \leq \bar{\rho}_i^S u_{t,i}; \forall t \in T, i \in I \tag{16}$$

$$0 \leq \rho_{t,i}^N \leq \bar{\rho}_i^N \mu_{t,i}; \forall t \in T, i \in I \tag{17}$$

$$\mu_{t,i} \leq 1 + u_{t,i} + \frac{\phi_{t,i} - \tau_i^-}{\tau_i^-}; \quad \forall t \in T, i \in I : \tau_i^- \neq 0 \tag{18}$$

$$\rho_{t,i}^S \leq (1-\gamma_{t,i})\bar{\rho}_{t,i}^S; \forall t \in T, i \in I \tag{19}$$

$$\rho_{t,i}^N \leq (1-\gamma_{t,i})\bar{\rho}_{t,i}^N; \forall t \in T, i \in I \tag{20}$$

$$\phi_{t,i} \leq 1 + \phi_{t-1,i}; \forall t \in T, i \in I \tag{21}$$

$$\phi_{t,i} \geq 1 + \phi_{t-1,i} - M u_{t,i}; \forall t \in T, i \in I \tag{22}$$

$$\phi_{t,i} \leq M \cdot (1 - u_{t,i}); \forall t \in T, i \in I \tag{23}$$

$$\phi_{t-1,i} \leq m_{t,i} + \sum_{k\in K: k<|K|} \bar{c}_{i,k}^T r_{t,i,k}; \forall t \in T, i \in I \tag{24}$$

$$m_{t,i} \leq M \cdot (r_{t,i,|K|} - s_{t,i} + 1); \forall t \in T, i \in I \tag{25}$$

$$\sum_{k\in K} r_{t,i,k} = s_{t,i}; \forall t \in T, i \in I \tag{26}$$

$$c_{t,i}^S = \sum_{k\in K} \bar{c}_{i,k}^S r_{t,i,k}; \forall t \in T, i \in I \tag{27}$$

$$\sum_{y=t-\tau_i^+}^{t} s_{y,i} \leq u_{t,i}; \forall t \in T, i \in I \tag{28}$$

$$\sum_{y=t-\tau_i^-}^{t} h_{y,i} \leq 1 - u_{t,i}; \forall t \in T, i \in I \tag{29}$$

$$s_{t,i} - h_{t,i} = u_{t,i} - u_{t-1,i}; \forall t \in T, i \in I \tag{30}$$

$$h_{t,i}, s_{t,i}, u_{t,i}, \gamma_{t,i} \in \{0,1\}; \forall t \in T, i \in I \tag{31}$$

$$r_{t,i,k} \in \{0,1\}; \forall t \in T, i \in I \tag{32}$$

$$\tilde{\rho}_t^S, \tilde{\rho}_t^N \geq 0; \forall t \in T \tag{33}$$

$$\phi_{t,i} \geq 0; \forall t \in T, i \in I. \tag{34}$$

Objective function (1) minimizes system-operation costs. We model non-wind generators as having three-part operating costs—start-up, no-load, and output-dependent variable costs. The variable costs, $c_i^V(\cdot)$, are convex piecewise-linear functions of the $q_{t,i}$'s, meaning that (1) is linear in the $q_{t,i}$'s. The final term in (1) penalizes load and reserve curtailments.

Constraints (2) and (3) ensure bus-level and system-wide load balance, respectively. Constraints (4) enforce flow limits on transmission lines.

Constraints (5)–(9) impose spinning- and non-spinning-reserve requirements. Constraints (5) define the values of the η_t^v's. Constraints (6) and (7) determine the generator that is the largest contingency during each hour, which is ensured by (19) and (20) not to supply reserves. Constraints (8) ensure that the total hourly reserve requirements are met. Constraints (9) ensure that a p.u. portion of the total reserve requirement is met by spinning reserves.

Constraints (10) ensure that each wind generator produces between zero and its maximum operating point, which depends on its hourly capacity factor (*i.e.*, wind conditions). Constraints (11)–(13) impose minimum and maximum production limits on non-wind generators. Constraints (12) and (13) account for additional power that is provided if reserves are called. Constraints (14) and (15) enforce ramping limits on each non-wind generator, accounting for reserves in determining upward ramping.

Constraints (16)–(20) restrict the provision of reserves. Constraints (16) and (17) ensure that no generator provides more reserves than it is capable of providing. $u_{t,i}$ and $\mu_{t,i}$ are included on the right-hand sides of (16) and (17), respectively, to ensure that generators provide spinning reserves only while they are online and that a generator does not provide non-spinning reserves if it is unable to start-up due to a minimum-down-time constraint. Constraints (18) determine the values of the $\mu_{t,i}$'s based on the number of hours that generators are scheduled to be offline and their minimum down times.

Constraints (21)–(23) define the number of hours that each non-wind generator is offline. If $u_{t,i} = 1$, (23) forces $\phi_{t,i}$ to equal zero. Otherwise, if $u_{t,i} = 0$, (22) forces $\phi_{t,i}$ to equal $\phi_{t-1,i}+1$. Constraints (24)–(27) compute start-up costs. Constraints (24) and (25) determine the type of start-up that occurs during a given hour, based on the duration of time that a given unit has been offline. Constraints (26) ensure that exactly one start-up type is incurred each time that a unit is started and (27) computes the corresponding cost.

Constraints (28) and (29) enforce minimum-up-time and -down-time restrictions, respectively. Constraints (30) define the values of $s_{t,i}$ and $h_{t,i}$ based on intertemporal changes in $u_{t,i}$. Constraints (31) and (32) impose integrality restrictions and (33) and (34) impose non-negativity.

III. Model Implementation

A. Overview

We use a rolling-horizon approach to model system operations one hour at a time. In doing so, we distinguish two

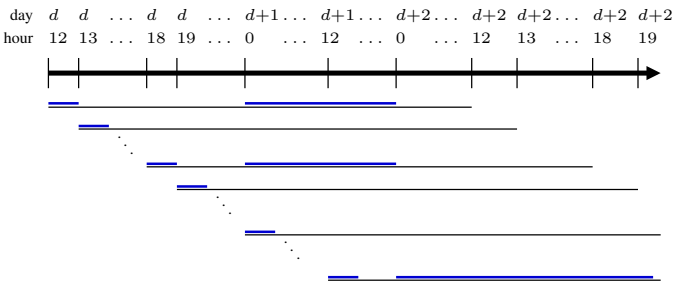

Fig. 1. Illustration of rolling-horizon modeling approach, assuming hour-12 and -18 unit commitment. The thin and thick lines indicate, respectively, the optimization horizon of and binding operational decisions that are made by the operational model that is solved during each hour.

processes. The first, to which we refer as unit commitment, determines the commitment schedule of non-wind generators for the following day as well as system operations for the current hour. The second, to which we refer as economic dispatch, determines current-hour system operations.

Figure 1 illustrates the sequence of these processes, for a case with unit commitment taking place during hours 12 and 18 during each day. The top of the figure labels the sequence of hours between hour 12 of day d and hour 19 of day $d+2$. The sets of lines below the horizontal time axis illustrate the optimization that takes place during each hour. Each thin line represents the model horizon of the optimization that is conducted during a given hour, whereas the thick lines represent the binding decisions that are made.

The first set of horizontal lines shows that unit commitment takes place during hour 12 of day d. This process determines the real-time operation of the system during hour 12 of day d, as well as day-$(d+1)$ unit commitments. These decisions are illustrated by hours that are covered by the thick lines. The thin line indicates that these decisions are made using a 48-hour optimization horizon through hour 12 of day $d+2$. These additional hours beyond day $d+1$ are included to ensure that sufficient generating capacity is kept online at the end of day $d+1$ to serve the day-$(d+2)$ load [37]. Including additional hours is especially important in operational planning of generators with high start-up costs and long minimum-up, minimum-down, and advanced-notification times.

Following the unit commitment that is conducted during hour 12 of day d, the decision-making process rolls forward sequentially through hours 13–17 of day d, conducting economic dispatch. These economic-dispatch processes determine system operation during each of these hours, using a rolling 48-hour optimization horizon. These economic-dispatch processes are followed by unit commitment during hour 18 of day d, which determines system operation during hour 18 of day d and can adjust day-$(d+1)$ unit-commitment decisions. These hourly optimization processes continue sequentially to simulate system operations over the full year.

B. Model Constraints

When modeling unit commitment, we impose the constraints:

$$u_{t,i} \geq \hat{u}_{t,i}; \forall t \in T, i \in I : t < \max\{\bar{t}, t_{\text{st}} + \theta_i\} \tag{35}$$

$$s_{t,i} = \hat{s}_{t,i}; \forall t \in T, i \in I : t < t_{\text{st}} + \theta_i; \tag{36}$$

where $\bar{t}$ is the final hour of the current day, θ_i is non-wind generator i's minimum notification time (h), and $\hat{s}_{t,i}$ and $\hat{u}_{t,i}$ are values of hour-t start-up and commitment decisions, respectively, of non-wind generator i that have been fixed during previous decision-making processes. Constraints (35) restrict the system operator's ability to shutdown units that are committed to be online by a previous unit commitment. Specifically, a unit that is scheduled to shutdown during the current day or before its minimum-notification time can be instructed instead to remain online as opposed to shutting down. Constraints (36) allow a unit to be started-up during the current or next day, so long as its minimum-notification time is respected.

We impose (36) and:

$$u_{t,i} \geq \hat{u}_{t,i}; \forall t \in T, i \in I; \tag{37}$$

on economic-dispatch processes. Constraints (37) are stricter variants of (35)—the only adjustment to unit-commitment instructions that (37) allow is starting-up units without the option of shutting-down units.

C. Algorithm

Algorithm 1 provides pseudocode that summarizes the steps of our rolling-horizon methodology. Line 1 takes as inputs values of h_i^0, q_i^0, u_i^0, ϕ_i^0, $\chi_i, \forall i \in I$, which give the starting state of each non-wind generator, and Δ, the number of days that are being simulated. χ_i is the number of hours that generator i has been online or offline (depending on whether it is positive or negative, respectively) as of the beginning of hour t_{st}. Line 2 initializes the algorithm by setting κ, which we use to compute total system-operation costs, equal to zero and fixing $\bar{t}$. Lines 3–32 are the main iterative loop, which cycle through the days of the year and hours of each day, which are indexed by y and h, respectively. Line 5 updates the starting and ending hours of the optimization horizon of the next decision-making process. Line 6 updates the starting state of each non-wind generator, based on the most recent model solution. Lines 7–13 impose minimum-up-time and -down-time restrictions, which are carried from the most recent model solution, on non-wind generators. Line 14 updates actual and forecasted wind-availability.

The decision-making process that is conducted in Lines 15–21 depends on whether h is an hour during which unit commitment or economic dispatch is conducted. T_U (*cf.* Line 15) represents the set of hours during which unit commitment is conducted. In the former case, the optimization is conducted including (35)–(36) in the model and commitment decisions are fixed (*cf.* Lines 17–18). In the latter case, the optimization is conducted including (36)–(37) in the model and no commitment decisions are fixed. Line 22 adds the operational cost that is incurred during hour h of day y to κ. Lines 23–30 update the ending state of each non-wind generator after the current decision-making process. This information is used in Lines 6–13 of the following iteration.

ξ^* in Lines 16 and 20 represents an optimal decision-variable vector. Optimal decision-variable values are used in

Algorithm 1 Rolling-Horizon Algorithm

1: **input:** h_i^0, q_i^0, u_i^0, ϕ_i^0, $\chi_i, \forall i \in I$; Δ
2: **initialize:** $\kappa \leftarrow 0$, $\bar{t} \leftarrow 23$
3: **for** $y \leftarrow 1$ to Δ **do**
4: **for** $h \leftarrow 0$ to 23 **do**
5: $t_{\text{st}} \leftarrow h$, $t_{\text{en}} \leftarrow h + 47$
6: $h_{t_{\text{st}}-1,i} \leftarrow h_i^0$, $q_{t_{\text{st}}-1,i} \leftarrow q_i^0$, $u_{t_{\text{st}}-1,i} \leftarrow u_i^0$, $\phi_{t_{\text{st}}-1,i} \leftarrow \phi_i^0, \forall i \in I$
7: **for** $i \in I$ **do**
8: **if** $\chi_i < 0$ **then**
9: fix $u_{t,i} = 0, \forall t \in T : t < \tau_i^- + \chi_i$
10: **else if** $\chi_i > 0$ **then**
11: fix $u_{t,i} = 1, \forall t \in T : t < \tau_i^+ - \chi_i$
12: **end if**
13: **end for**
14: update $\zeta_{t,i}, \forall t \in T, i \in \Omega$
15: **if** $h \in T_U$ **then**
16: $\xi^* \leftarrow \arg\min$ (1) s.t. (2)–(36)
17: $\hat{u}_{t,i} \leftarrow u^*_{t,i}, \forall t \in T, i \in I : t > \bar{t}$
18: $\hat{s}_{t,i} \leftarrow s^*_{t,i}, \forall t \in T, i \in I : t > \bar{t}$
19: **else**
20: $\xi^* \leftarrow \arg\min$ (1) s.t. (2)–(34), (36)–(37)
21: **end if**
22: $\kappa \leftarrow \kappa + \sum_{i \in I} \left[c^{S*}_{t_{\text{st}},i} + c_i^N u^*_{t_{\text{st}},i} + c_i^V(q^*_{t_{\text{st}},i}) \right]$
23: $h_i^0 \leftarrow h^*_{t_{\text{st}},i}$, $q_i^0 \leftarrow q^*_{t_{\text{st}},i}$, $u_i^0 \leftarrow u^*_{t_{\text{st}},i}$, $\phi_i^0 \leftarrow \phi^*_{t_{\text{st}},i}$, $\forall i \in I$
24: **for** $i \in I$ **do**
25: **if** $u^*_{t_{\text{st}},i} = 1$ **then**
26: $\chi_i \leftarrow \max\{\chi_i + 1, 1\}$
27: **else**
28: $\chi_i \leftarrow \min\{\chi_i - 1, -1\}$
29: **end if**
30: **end for**
31: **end for**
32: **end for**

fixing unit-commitment decisions in Lines 17–18, computing operational cost in Line 22, and updating the state of non-wind generators in Lines 23–30.

IV. Example

This section presents a stylized two-day example, which demonstrates the tradeoffs in the timing of conducting recommitment. Table I summarizes data for the eight dispatchable generators that are modeled in the example. There is an additional 1000-MW wind plant. Generators 1–4 are relatively flexible, in that they require no advanced notification to start-up, can ramp over their full operating range within a single hour, and have no minimum-up-time requirements. These units are relatively costly to operate. Generators 5–8 are relatively inflexible, requiring seven hours of advanced notification time to start-up, have minimum up-times of two or four hours, and are able to ramp over one quarter of their operating range within a single hour. These units are relatively inexpensive to operate. Constraint parameters that are not listed in Table I are neglected in the example, as are reserve and transmission-network constraints.

TABLE I
Dispatchable-Generator Data for Example from Section IV

i	θ_i	K_i^+	τ_i^+	R_i^+	c_i^V	c_i^N	$\bar{c}^S_{i,1}$
1	0	100	1	100	1000	1000	10000
2	0	100	1	100	1000	1000	10000
3	0	100	1	100	1000	1000	10000
4	0	100	1	100	1000	1000	10000
5	7	100	4	25	100	100	1000
6	7	100	4	25	100	100	1000
7	7	100	4	25	100	100	1000
8	7	100	2	25	100	100	1000

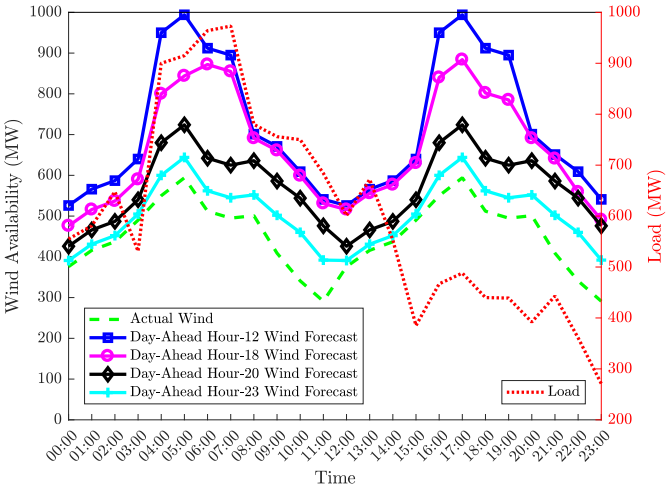

Fig. 2. Modeled load and actual wind availability during the second day of the example from Section IV and day-ahead wind-availability forecasts produced during hours 12, 18, 20, and 23 of the first day.

Figure 2 summarizes the assumed load and actual wind availability during the second day of the example, as well as wind-availability forecasts that are produced during hours 12, 18, 20, and 23 of the first day. The forecasts overestimate wind availability, with the hour-23 forecast being the most accurate.

Table II summarizes optimized generator commitments, as of hour 12 of the first day, for the first 14 hours of the second day. Because they are relatively costly, units 1–4 are not committed and the system relies upon units 5–8 to supplement forecasted wind production. The hour-12 day-ahead wind-availability forecast, which is used to determine the commitments that are summarized in Table II, overestimates wind availability. As such, additional units must be committed, either day-ahead (if recommitment is conducted) or in real time.

Table III summarizes the impact of recommitment. The first row of Table III reports the total number of the first 14 hours of the second day during which each unit is committed without recommitment (*i.e.*, the sums of the values that are reported in Table II). The remaining rows of Table III show that if the system is recommitted, more generators (especially relatively low-cost units 5–8) are scheduled to operate during the second day. These changed commitments arise from the improved forecasts that are available later during the day (*cf.* Fig. 2). Although the hour-23 wind-availability forecast is the most accurate, hour-23 recommitment results in units 1–4

TABLE II
GENERATOR COMMITMENTS, AS OF HOUR 12 OF THE FIRST DAY, DURING FIRST 14 HOURS OF SECOND DAY OF EXAMPLE FROM SECTION IV

	Hour													
i	0	1	2	3	4	5	6	7	8	9	10	11	12	13
1	0	0	0	0	0	0	0	0	0	0	0	0	0	0
2	0	0	0	0	0	0	0	0	0	0	0	0	0	0
3	0	0	0	0	0	0	0	0	0	0	0	0	0	0
4	0	0	0	0	0	0	0	0	0	0	0	0	0	0
5	1	1	1	0	0	0	0	0	0	0	0	0	0	0
6	0	0	0	0	0	0	1	1	1	1	1	1	1	1
7	0	0	0	0	0	0	0	0	0	0	0	0	0	0
8	0	1	1	0	0	1	1	1	1	1	1	1	1	1
9	1	1	1	1	1	1	1	1	1	1	1	1	1	1

TABLE III
NUMBER OF THE FIRST 14 HOURS OF SECOND DAY OF EXAMPLE FROM SECTION IV THAT EACH GENERATOR IS COMMITTED DAY-AHEAD WITH UNIT COMMITMENT CONDUCTED AT DIFFERENT TIMES

	i							
Unit-Commitment Hours	1	2	3	4	5	6	7	8
12	0	0	0	0	3	8	0	11
12 and 18	0	0	0	0	5	10	0	14
12 and 20	0	0	0	0	8	10	10	14
12 and 23	1	0	2	4	8	8	8	14

being committed day-ahead. These units must be committed because units 5–8 cannot be committed during the early hours of the second day without violating their notification-time constraints.

Table IV summarizes the total number of the first 14 hours of the second day that each unit *actually* is committed, with different recommitment times. Differences between the values that are reported in Tables III and IV reflect some units having to be committed in real time to correct for errors in wind-availability forecasts. Not conducting a day-ahead recommitment results in the greatest use of the relatively high-cost units 1–4 for a total of 19 hours. Conversely, an hour-20 recommitment requires the use of these costly units for only a total of eight hours. Conducting an hour-23 recommitment requires the use of the relatively costly units for a total of 12 hours, because some less-costly units cannot be committed without violating their notification-time constraints.

Table V summarizes the impacts of these different commitments on the dispatch of the generating fleet. The first two rows show that when the hour-12 day-ahead unit commitment is conducted, 9411 MWh of wind is forecasted to be available during the first 14 hours of the second day. The remaining 899 MWh of load is scheduled to be served using units 5–8. However, only 6095 MWh of wind actually is available, meaning that the 3316-MWh deficit must be covered by the balance of the generating fleet. Units 5–8 are able to increase their production 2116 MWh relative to their day-ahead schedules. However, 1200 MWh of load must be covered by units 1–4.

TABLE IV
ACTUAL NUMBER OF THE FIRST 14 HOURS OF SECOND DAY OF EXAMPLE FROM SECTION IV THAT EACH GENERATOR IS COMMITTED WITH UNIT COMMITMENT CONDUCTED AT DIFFERENT TIMES

	i							
Unit-Commitment Hours	1	2	3	4	5	6	7	8
12	4	3	7	5	14	8	0	14
12 and 18	0	4	10	1	14	10	0	14
12 and 20	4	0	1	3	12	10	10	14
12 and 23	3	1	4	4	12	8	8	14

TABLE V
SCHEDULED AND ACTUAL DISPATCH OF GENERATORS (MWH) OVER THE FIRST 14 HOURS OF SECOND DAY OF EXAMPLE FROM SECTION IV WITH UNIT COMMITMENT CONDUCTED AT DIFFERENT TIMES

Unit-Commitment Hours		Units 1–4	Units 5–8	Wind Generator
12	Scheduled	0	899	9411
	Actual	1200	3015	6095
12 and 18	Scheduled	0	1356	8954
	Actual	968	3247	6095
12 and 20	Scheduled	0	2746	7564
	Actual	372	3843	6095
12 and 23	Scheduled	486	3090	6734
	Actual	722	3493	6095

The remaining rows of Table V show that conducting recommitment later during the day allows more generating capacity from units 5–8 to be scheduled, because of the improved wind-availability forecasts. However, in all cases, some energy is produced in real time by units 1–4, because there are errors in the wind-availability forecasts that must be balanced. Moreover, more production from units 1–4 must be scheduled when conducting an hour-23 recommitment, because notification-time constraints do not allow changing the commitments of units 5–8 during the early hours of the second day.

Table VI summarizes the actual cost of operating the system during the second day of the example, with different unit-commitment times. The cost trends follow the results that are summarized in Tables II–V. Recommitting the system later in the day is beneficial. Without recommitment, a substantial portion of wind-supply deficits must be served using units 1–4. Recommitment allows lower-cost inflexible units to be committed, once an updated forecast indicates less wind being available. Although the hour-23 wind-availability forecast is the most accurate, notification-time constraints limit adjustments to the commitments of units 5–8. This result shows a tradeoff between forecast accuracy and generator flexibility in determining when to conduct recommitment.

V. CASE-STUDY DATA AND BENCHMARKING

A. Case-Study Data

Our case study is based on ISO New England, from which conventional-generator and transmission-network data are obtained directly. Previous works [38]–[41] detail these datasets. We model a total of 276 non-wind generators, which represent

TABLE VI
ACTUAL OPERATION COST ($) DURING SECOND DAY OF EXAMPLE FROM SECTION IV WITH UNIT COMMITMENT CONDUCTED AT DIFFERENT TIMES

Unit-Commitment Hour	Operation Cost
12	249 490
12 and 18	204 140
12 and 20	146 650
12 and 23	193 860

TABLE VII
SUM OF SQUARED ERRORS BETWEEN MODELED ACTUAL AND UNSHIFTED AND SHIFTED FORECASTED WIND AVAILABILITIES AND TIME SHIFT USED FOR CASE STUDY FROM SECTION VI

Forecast Horizon (Hours Ahead)	Sum of Squared Errors		Time Shift (h)
	Unshifted	Shifted	
1	330	25	2
4	321	282	2
6	381	379	1
24	405	405	0

31.44 GW of nameplate capacity. Generators are modeled as having three start-up types—hot, intermediate, and cold. We assume that $\eta = 0.07$ and $\eta^S = 0.5$.

Hourly historical year-2009 load data for the eight load zones in ISO New England are obtained from a public repository.[2] The system-wide load ranges between 8.90 GW and 24.73 GW and averages 14.26 GW across the year.

We model cases with two wind penetrations—4.32 GW and 6.48 GW of nameplate capacity, which are 17.0% and 25.5%, respectively, of peak load. These cases correspond to wind serving 13.0% and 19.5%, respectively, of annual load (absent wind curtailment). Wind capacities (*i.e.*, the value of $Z_i, \forall i \in \Omega$) for the two wind-penetration levels are apportioned to the eight load zones in proportion to their co-incident peak loads.

Actual hourly wind availability and forecasts of such (*i.e.*, the values of $\zeta_{t,i}, \forall t \in T, i \in \Omega$) are modeled using data from Wind Integration National Dataset (WIND) Toolkit [42]–[44]. WIND Toolkit includes modeled actual wind availability and forecasts of such for wind turbines with 100-m hub heights at 126 000 sites across the continental U.S. for the years 2007–2013. We use these data for the year 2009 to capture correlations between load and weather conditions.

We employ a two-step process to model $\zeta_{t,i}, \forall t \in T, i \in \Omega$. First, each set of modeled actual and forecasted wind-availability data are averaged across each of the eight load zones to determine a zonal-average capacity factor. We do this by computing the simple average of the capacity factors that are reported in WIND Toolkit for sites that are in each of the eight zones. Next, the modeled actual and forecasted wind-availability data are used to determine the values of $\zeta_{t,i}, \forall t \in T, i \in \Omega$. For a given instance of model (1)–(34), the values of $\zeta_{t_{\text{st}},i}, \forall i \in \Omega$ are set equal to the corresponding zonal-average modeled *actual* capacity factor for the hour. For the remaining hours, $t > t_{\text{st}}$, we use zonal-average *forecasted* capacity factors. WIND Toolkit provides 1-, 4-, 6-, and 24-hour-ahead forecasts of wind availability. We use weighted-averages of these forecasted capacity factors to set values of $\zeta_{t,i}, \forall t > t_{\text{st}}, i \in \Omega$. For instance, the value of $\zeta_{t_{\text{st}}+4,i}, \forall i \in \Omega$ is set equal to the 4-hour-ahead forecasted wind availability for the corresponding hour, whereas the value of $\zeta_{t_{\text{st}}+7,i}, \forall i \in \Omega$ is set equal to the weighted average of the 6- and 24-hour-ahead forecasted wind availabilities for the corresponding hour, with weights of $17/18$ and $1/18$, respectively. Values of $\zeta_{t,i}, \forall t \geq t_{\text{st}} + 24, i \in \Omega$ are set equal to the 24-hour-ahead forecast.

[2]https://www.iso-ne.com/isoexpress/web/reports/load-and-demand/

One peculiarity of WIND Toolkit, which is summarized in Table VII, is that the forecasts do not become more accurate as they are produced closer to real-time. The first two columns of Table VII show that 1-hour-ahead forecasts have higher forecast errors than 4-hour-ahead forecasts do. Following consultation with members of the WIND Toolkit team at National Renewable Energy Laboratory, we follow their suggestion and correct the error by time-shifting each set of wind-availability forecasts to minimize its sum of squared errors with the modeled actual wind availabilities. The final two columns of Table VII summarize the optimal time shifts of the forecasts and the resulting sum of squared errors.

B. Benchmarking and Cases Examined

We focus on the impacts of recommitment on operational wind-integration costs. Thus, we model wind availability as the sole source of uncertainty. This uncertainty is reflected by the values of $\zeta_{t,i}, \forall t \in T, i \in \Omega$ being updated iteratively as operational decisions are made (*cf.* Line 14 of Algorithm 1). We contrast system-operation costs with uncertain $\zeta_{t,i}, \forall t \in T, i \in \Omega$ to a perfect-foresight benchmark, in which Algorithm 1 is used but $\zeta_{t,i}$ is equal to its modeled actual value $\forall t \in T, i \in \Omega$ in each unit-commitment and economic-dispatch model. Comparing costs with and without wind uncertainty is a standard approach to measuring operational wind-integration costs [9].

In addition to considering cases with two wind-penetration levels (4.32 GW and 6.48 GW), we consider cases with base and low levels of generator flexibility. Base flexibility uses the values of $\theta_i, \forall i \in I$ that are reported in the ISO New England dataset. Low flexibility uses doubled values of $\theta_i, \forall i \in I$.

We contrast a case in which unit commitment is conducted during noon of each day to cases in which unit commitment is conducted during noon and during some combination of hours 18, 20, and 23, giving seven combinations total.

VI. CASE-STUDY RESULTS

Figure 3 summarizes modeled actual system-wide wind availability during the first 12 hours of 10 January, 2009 and three different day-ahead wind-availability forecasts. The figure assumes the base case of 4.32 GW of wind capacity. Figure 3 shows that the forecasts overestimate wind availability for the most part. The forecast that is produced at noon has the greatest overall errors—overestimating wind availability during the first hour of 10 January, 2009 by over 400%. The forecast that is produced during hour 23 is the most accurate.

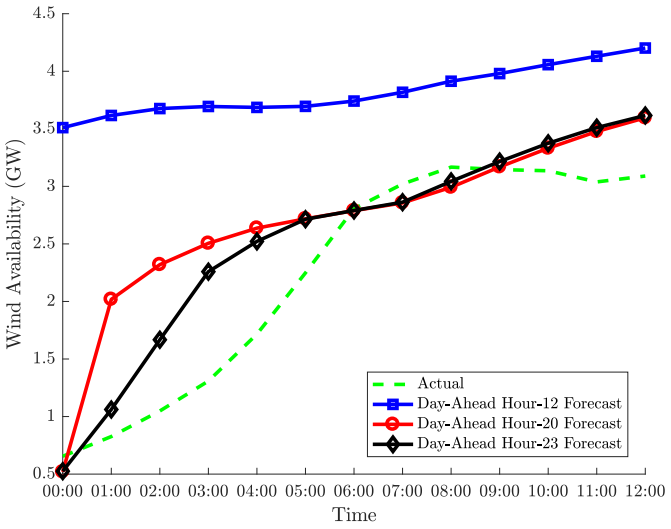

Fig. 3. Modeled actual system-wide wind availability during the first 12 hours of 10 January, 2009 and corresponding day-ahead forecasts produced during hours 12, 20, and 23 of 9 January, 2009 assuming 4.32 GW of wind for case study from Section VI.

TABLE VIII
TOTAL ($ MILLION) AND P.U. ($/MWH) SYSTEM-OPERATION COSTS DURING 10 JANUARY, 2009 WITH UNIT COMMITMENT CONDUCTED AT DIFFERENT TIMES ASSUMING 4.32 GW OF WIND AND BASE GENERATOR FLEXIBILITY FOR CASE STUDY FROM SECTION VI

Unit-Commitment Hours	12	12 and 20	12 and 23
Total Cost	7.06	6.81	6.88
Per-MWh Cost	190	183	185

System operations differ, depending on whether only a noon day-ahead unit commitment is conducted or recommitment is conducted also. With only noon day-ahead unit commitment, assuming base generator flexibility, the energy-supply shortfall that arises in real time from actual wind production being lower than the noon forecast is addressed by committing 32 fast-start generators in real time (beginning during hour 0 of 10 January, 2009), which operate for a total of 80 hours between them. These fast-start units have high operating costs, which increases operating cost for the day. Table VIII summarizes the total and per-MWh cost of operating the system during 10 January, 2009, using only noon day-ahead unit commitment or noon day-ahead unit commitment that is followed by either hour-20 or -23 recommitment.

Conducting hour-20 or -23 recommitment reduces the total number of hours that the 32 fast-start units are operated to 70 and 68 hours, respectively. These fast-start units are replaced by lower-cost units that require advanced notification to start-up. Table VIII shows that reduced use of fast-start units results in up to 4% cost decreases in these cases relative to conducting only noon day-ahead unit commitment.

We illustrate the high cost of fast-start units by computing:

$$\tilde{c}_i^V = \frac{c_i^V(K_i^+)}{K_i^+}; \forall i \in I;$$

which is the average output-dependent cost of each unit, if it operates at its nameplate capacity. Table IX summarizes the capacity-weighted averages of the values of $\tilde{c}_i^V$ corresponding to generators that are grouped based on θ_i. Relatively flexible generators, with advanced-notification times of four hours or less are, on average, up to 13 times as costly to operate, relative to generators with higher advanced-notification times.

TABLE IX
CAPACITY-WEIGHTED AVERAGE OF $\tilde{c}_i^V$ FOR θ_i-BASED GROUPINGS OF GENERATORS ASSUMING BASE GENERATOR FLEXIBILITY FOR CASE STUDY FROM SECTION VI

θ_i	≤ 4	5–8	9–12	≥ 13
Capacity-Weighted Average of $\tilde{c}_i^V$	324	91	64	25

TABLE X
COST AND FLEXIBILITY DATA FOR THREE UNITS FROM CASE STUDY FROM SECTION VI THAT ARE OPERATED DIFFERENTLY BETWEEN HOUR-20 AND -23 RECOMMITMENT ASSUMING BASE GENERATOR FLEXIBILITY

i	46	191	256
θ_i	8	0	2
$\tilde{c}_i^V$	52	263	186

If conducting only a noon day-ahead unit commitment, the system relies heavily on units with advanced-notification times of four hours or less to meet the wind-availability deficit. This reliance stems from the inability to commit lower-cost units with longer advanced-notification times. Conversely, with hour-20 recommitment these most expensive units can be substituted to some extent by lower-cost units that have higher advanced-notification times.

Figure 3 shows that the wind-availability forecast that is produced during hour 23 is more accurate than that which is produced during hour 20. However, hour-20 recommitment reduces operating cost relative to hour-23 recommitment. This cost savings stems from the hour-23 recommitment being 'too late' in the sense that although the hour-23 forecast is more accurate, low-cost units cannot be committed to operate during the early hours of 10 January, 2009, due to the advanced-notification times. This finding demonstrates a fundamental tradeoff in determining when to conduct recommitment—later unit commitment has access to more accurate wind-availability forecasts, but a more limited set of generators that can be committed, given their flexibility constraints.

To illustrate this tradeoff, we focus on the operation during the first 12 hours of 10 January, 2009 of three units, the cost and flexibility characteristics of which are summarized in Table X. The three units display the tradeoff between flexibility and cost that is summarized in Table IX. With hour-20 recommitment, generator 46, which is the lowest-cost of the three, is operated during hours 6–12 and generator 256 is operated during hours 8–12. With hour-23 recommitment, generator 46 cannot be started-up until hour 8 (due to its notification-time requirement). Thus, generator 256 must be operated during hours 6–12 and generator 191 must be operated during hours 6–7.

Tables XI and XII summarize operational wind-uncertainty

TABLE XI
OPERATIONAL WIND-INTEGRATION COSTS FOR CASE STUDY FROM SECTION VI ($/MWH OF WIND PRODUCED)

	Wind Penetration	Low	High	Low	High
	Flexibility	Base	Base	High	High
Unit-Commitment Hours	12	1.49	3.18	1.49	3.18
	12 and 18	1.41	3.05	1.47	3.13
	12 and 20	1.33	2.83	1.34	2.89
	12 and 23	1.34	3.02	1.39	3.07
	12, 18, and 20	1.24	2.69	1.31	2.79
	12, 18, and 23	1.31	2.76	1.36	2.93
	12, 20, and 23	1.27	2.72	1.33	2.86
	12, 18, 20, and 23	1.22	2.62	1.30	2.75

TABLE XII
PERCENTAGE REDUCTION IN OPERATIONAL WIND-INTEGRATION COSTS RELATIVE TO NOON DAY-AHEAD UNIT COMMITMENT ONLY FOR CASE STUDY FROM SECTION VI

	Wind Penetration	Low	High	Low	High
	Flexibility	Base	Base	Low	Low
Unit-Commitment Hours	12 and 18	5	4	1	3
	12 and 20	10	11	10	9
	12 and 23	10	5	6	3
	12, 18, and 20	16	16	12	12
	12, 18, and 23	12	13	8	8
	12, 20, and 23	15	14	11	11
	12, 18, 20, and 23	18	18	13	14

costs for the four different cases that we examine with different wind-penetration and generator-flexibility levels and day-ahead unit commitment conducted during different hours. Table XI reports wind-uncertainty costs that are normalized by total wind production when using wind-availability forecasts. Table XII reports the percentage decrease in operational wind-uncertainty costs relative to conducting a noon day-ahead unit commitment only. The tables show two results, which our detailed analysis of 10 January, 2009 suggests.

First, if conducting a single recommitment, an hour-20 recommitment yields the greatest cost reductions. This result keeps with our finding a tradeoff between forecast accuracy and generator flexibility. Conducting three recommitments yields further cost reduction and two recommitments yields cost reductions in most cases. With low generator flexibility, hour-20 recommitment yields slightly lower costs compared to hours-18 or -23 recommitments. This result stems from the combined impact of relatively (to hour-20) inaccurate hour-18 wind-availability forecasts and the system having limited operational flexibility during hour 23.

Tables XI and XII show that increasing wind penetration or decreasing generator flexibility increases operational wind-integration costs. Higher wind penetrations mean that forecast errors yield larger absolute supply/demand imbalances. Increasing the wind penetration by 50% more than doubles operational wind-integration costs. Increasing the penetration of wind further should lead to further cost escalations. Less flexible dispatchable generators require that the system operator provides additional notification to commit inflexible low-cost units. Recommitment gives reduced cost savings with less-flexible generators, because there are fewer options to commit low-cost generators. With doubled advanced-notification times, hour-20 recommitment gives the greatest cost savings. Should the generation fleet become sufficiently inflexible, hour-18 recommitment may provide a better tradeoff between forecast accuracy and generator flexibility than hour-20 recommitment does. Algorithm 1 is computationally costly, because system operations are re-optimized hourly across the full year. Each model in Lines 16 and 20 of Algorithm 1 has over 720 097 variables and 600 691 constraints, respectively, and a median solution time of 25.7 s of wall-clock time. Thus, we do not examine cases with higher advanced-notification times than the low-flexibility case in which $\forall i \in I, \theta_i$ is doubled relative to the ISO New England data.

VII. CONCLUSIONS

This paper examines the benefits of recommitment in reducing operational wind-uncertainty costs. To do so, we develop a detailed operational model that mimics many of the costs and constraints for which system operators account in their operational models. Nonetheless, our model is not an exact replica of that used by any market operator. We develop a rolling-horizon algorithm to simulate hourly system operations that consist of unit commitment and economic dispatch. The key distinction between these processes is the extent to which the system operator can adjust commitment decisions relative to previous decisions and which decisions are binding.

We demonstrate our model and draw important conclusions regarding the use of recommitment with a comprehensive case study, which is based on ISO New England, and a stylized example. Both the example and case study demonstrate the cost impacts of wind uncertainty, which are increasing in wind penetration and generator inflexibility. We demonstrate also the benefits of introducing recommitment, which raises a fundamental tradeoff between forecast accuracy and operational flexibility. For our example and case study, hour-20 recommitment offers the most cost reductions. Other systems may benefit from recommitment being conducted at different times and the methodology that we develop could be used to examine the tradeoffs therein.

We adopt an hourly timescale for all of our modeling. Hourly timescales are used in nearly all wholesale electricity markets for day-ahead and reliability unit commitment. With few exceptions, sub-hourly timescales are used for economic-dispatch modeling. We use an hourly timescale for our economic-dispatch modeling, due to the computational cost that sub-hourly timescales would entail. Modeling economic dispatch at sub-hourly timescales could reveal more load and wind-availability variability (compared to hourly timescales). However, our fundamental results regarding the tradeoffs in introducing and the timing of recommitment likely would continue to hold.

Our model does not allow wind generators to provide reserves, *e.g.*, if their output is curtailed. An area of future study could examine the benefits of using curtailed wind in this manner. Another area of future work would be to compare the benefits of recommitment to a modeling paradigm

that represents uncertainty explicitly, *e.g.*, stochastic, robust, chance-constrained, or distributionally robust optimization. We do not consider explicit uncertainty representation, because no wholesale market employs such a model today [35], [36]. Thus, this assumption is keeping with our goal of understanding how current *deterministic* market models could be improved to accommodate wind uncertainty.

ACKNOWLEDGMENT

The authors thank the editors, four anonymous reviews, A. J. Conejo, A. Sorooshian, and D. Koohmarey for helpful discussions, suggestions, and comments.

REFERENCES

[1] J. E. Bistline, "Economic and technical challenges of flexible operations under large-scale variable renewable deployment," *Energy Economics*, vol. 64, pp. 363–372, May 2017.

[2] R. Sioshansi and W. Short, "Evaluating the Impacts of Real-Time Pricing on the Usage of Wind Generation," *IEEE Transactions on Power Systems*, vol. 24, pp. 516–524, May 2009.

[3] J. DeCesaro and K. Porter, "Wind Energy and Power System Operations: A Review of Wind Integration Studies to Date," National Renewable Energy Laboratory, Golden, CO, Tech. Rep. NREL/SR-550-47256, December 2009.

[4] J. Dowds, P. Hines, T. Ryan, W. Buchanan, E. Kirby, J. Apt, and P. Jaramillo, "A review of large-scale wind integration studies," *Renewable and Sustainable Energy Reviews*, vol. 49, pp. 768–794, September 2015.

[5] A. Bloom, A. Townsend, D. Palchak, J. Novacheck, J. King, C. Barrows, E. Ibanez, M. O'Connell, G. Jordan, B. Roberts, C. Draxl, and K. Gruchalla, "Eastern Renewable Generation Integration Study," National Renewable Energy Laboratory, Golden, CO, Tech. Rep. NREL/TP-6A20-64472, August 2016.

[6] "Western Wind and Solar Integration Study," National Renewable Energy Laboratory, Golden, CO, Tech. Rep. NREL/SR-550-47434, May 2010.

[7] D. Lew, G. Brinkman, E. Ibanez, A. R. Florita, M. Heaney, B.-M. Hodge, M. Hummon, G. B. Stark, J. King, S. A. Lefton, N. Kumar, D. Agan, G. A. Jordan, and S. Venkataraman, "The Western Wind and Solar Integration Study Phase 2," National Renewable Energy Laboratory, Golden, CO, Tech. Rep. NREL/TP-5500-55588, September 2013.

[8] N. W. Miller, M. Shao, S. Pajic, and R. D'Aquila, "Western Wind and Solar Integration Study Phase 3 — Frequency Response and Transient Stability," National Renewable Energy Laboratory, Golden, CO, Tech. Rep. NREL/SR-5D00-62906, December 2014.

[9] R. Sioshansi, "Evaluating the Impacts of Real-Time Pricing on the Cost and Value of Wind Generation," *IEEE Transactions on Power Systems*, vol. 25, pp. 741–748, April 2010.

[10] S. H. Madaeni and R. Sioshansi, "Measuring the Benefits of Delayed Price-Responsive Demand in Reducing Wind-Uncertainty Costs," *IEEE Transactions on Power Systems*, vol. 28, pp. 4118–4126, November 2013.

[11] A. Alahäivälä, J. Ekström, J. Jokisalo, and M. Lehtonen, "A framework for the assessment of electric heating load flexibility contribution to mitigate severe wind power ramp effects," *Electric Power Systems Research*, vol. 142, pp. 268–278, January 2017.

[12] F. S. Gazijahani and J. Salehi, "IGDT-Based Complementarity Approach for Dealing With Strategic Decision Making of Price-Maker VPP Considering Demand Flexibility," *IEEE Transactions on Industrial Informatics*, vol. 16, pp. 2212–2220, April 2020.

[13] A. Castillo and D. F. Gayme, "Grid-scale energy storage applications in renewable energy integration: A survey," *Energy Conversion and Management*, vol. 87, pp. 885–894, November 2014.

[14] S. W. Alnaser and L. F. Ochoa, "Optimal Sizing and Control of Energy Storage in Wind Power-Rich Distribution Networks," *IEEE Transactions on Power Systems*, vol. 31, pp. 2004–2013, May 2016.

[15] T. Edmunds, A. Lamont, V. Bulaevskaya, C. Meyers, J. Mirocha, A. Schmidt, M. Simpson, S. Smith, P. Sotorrio, P. Top, and Y. Yao, "The Value of Energy Storage and Demand Response for Renewable Integration in California," California Energy Commission, Tech. Rep. CEC-500-2017-014, February 2017.

[16] D. Stenclik, P. Denholm, and B. Chalamala, "Maintaining Balance: The Increasing Role of Energy Storage for Renewable Integration," *IEEE Power and Energy Magazine*, vol. 15, pp. 31–39, November-December 2017.

[17] R. Sioshansi, P. Denholm, J. Arteaga, S. Awara, S. Bhattacharjee, A. Botterud, W. Cole, A. Cortés, A. de Queiroz, J. DeCarolis, Z. Ding, N. DiOrio, Y. Dvorkin, U. Helman, J. X. Johnson, I. Konstantelos, T. Mai, H. Pandžić, D. Sodano, G. Stephen, A. Svoboda, H. Zareipour, and Z. Zhang, "Energy-Storage Modeling: State-of-the-Art and Future Research Directions," *IEEE Transactions on Power Systems*, 2021, in press.

[18] V. Marano and G. Rizzoni, "Energy and Economic Evaluation of PHEVs and their Interaction with Renewable Energy Sources and the Power Grid," in *2008 IEEE International Conference on Vehicular Electronics and Safety*. Columbus, OH, USA: Institute of Electrical and Electronics Engineers, September 2008.

[19] H. Lund and W. Kempton, "Integration of renewable energy into the transport and electricity sectors through V2G," *Energy Policy*, vol. 36, pp. 3578–3587, September 2008.

[20] A. Papavasiliou and S. S. Oren, "Coupling Wind Generators with Deferrable Loads," in *Energy 2030 Conference*. Atlanta, GA, USA: Institute of Electrical and Electronics Engineers, 17-18 November 2008.

[21] C. Weiller and R. Sioshansi, "The Role of Plug-In Electric Vehicles with Renewable Resources in Electricity Systems," *Revue d'économie industrielle*, vol. 148, pp. 291–316, 2014.

[22] S. Chandrashekar, Y. Liu, and R. Sioshansi, "Wind-Integration Benefits of Controlled Plug-In Electric Vehicle Charging," *Journal of Modern Power Systems and Clean Energy*, vol. 5, pp. 746–756, September 2017.

[23] S. J. Deng and S. S. Oren, "Electricity derivatives and risk management," *Energy*, vol. 31, pp. 940–953, May-June 2006.

[24] D. Xiao, M. K. AlAshery, and W. Qiao, "Optimal Price-Maker Trading Strategy of Wind Power Producer using Virtual Bidding," *Journal of Modern Power Systems and Clean Energy*, 2021, in press.

[25] S. H. Madaeni and R. Sioshansi, "The Impacts of Stochastic Programming and Demand Response on Wind Integration," *Energy Systems*, vol. 4, pp. 109–124, June 2013.

[26] Q. P. Zheng, J. Wang, and A. L. Liu, "Stochastic Optimization for Unit Commitment—A Review," *IEEE Transactions on Power Systems*, vol. 30, pp. 1913–1924, July 2015.

[27] S. Y. Abujarad, M. W. Mustafa, and J. J. Jamian, "Recent approaches of unit commitment in the presence of intermittent renewable energy resources: A review," *Renewable and Sustainable Energy Reviews*, vol. 70, pp. 215–223, April 2017.

[28] M. Håberg, "Fundamentals and recent developments in stochastic unit commitment," *International Journal of Electrical Power & Energy Systems*, vol. 109, pp. 38–48, July 2019.

[29] S. Torabzadeh, M. J. Feizollahi, and S. Mousavian, "Robust Unit Commitment and the Promise of Higher Reliability in Electricity Markets," *Current Sustainable/Renewable Energy Reports*, vol. 6, pp. 90–99, September 2019.

[30] X. Zheng, K. Qu, J. Lv, Z. Li, and B. Zeng, "Addressing the Conditional and Correlated Wind Power Forecast Errors in Unit Commitment by Distributionally Robust Optimization," *IEEE Transactions on Sustainable Energy*, vol. 12, pp. 944–954, April 2021.

[31] A. Tuohy, E. Denny, and M. O'Malley, "Rolling Unit Commitment for Systems with Significant Installed Wind Capacity," in *2007 IEEE Lausanne Power Tech*. Lausanne, Switzerland: Institute of Electrical and Electronics Engineers, 1-5 July 2007.

[32] A. Tuohy, P. Meibom, E. Denny, and M. O'Malley, "Unit Commitment for Systems With Significant Wind Penetration," *IEEE Transactions on Power Systems*, vol. 24, pp. 592–601, May 2009.

[33] P. Carpentier, G. Gohen, J.-C. Culioli, and A. Renaud, "Stochastic optimization of unit commitment: a new decomposition framework," *IEEE Transactions on Power Systems*, vol. 11, pp. 1067–1073, May 1996.

[34] G. Pritchard, G. Zakeri, and A. Philpott, "A Single-Settlement, Energy-Only Electric Power Market for Unpredictable and Intermittent Participants," *Operations Research*, vol. 58, pp. 1210–1219, July-August 2010.

[35] M. Musto, "Day Ahead Network Constrained Unit Commitment Performance," in *Eleventh Annual FERC Software Conference*. Washington, DC: Institute of Electrical and Electronics Engineers, 23-25 June 2020.

[36] B. Knueven, J. Ostrowski, and J.-P. Watson, "On Mixed-Integer Programming Formulations for the Unit Commitment Problem," *INFORMS Journal on Computing*, vol. 32, pp. 857–876, Fall 2020.

[37] S. H. Madaeni and R. Sioshansi, "Using Demand Response to Improve the Emission Benefits of Wind," *IEEE Transactions on Power Systems*, vol. 28, pp. 1385–1394, May 2013.

[38] R. Sioshansi, R. P. O'Neill, and S. S. Oren, "Economic Consequences of Alternative Solution Methods for Centralized Unit Commitment in Day-Ahead Electricity Markets," *IEEE Transactions on Power Systems*, vol. 23, pp. 344–352, May 2008.
[39] R. Sioshansi, S. S. Oren, and R. P. O'Neill, "The Cost of Anarchy in Self-Commitment Based Electricity Markets," in *Competitive Electricity Markets: Design, Implementation & Performance*, F. P. Sioshansi, Ed. Elsevier, 2008.
[40] R. Sioshansi, S. S. Oren, and R. O'Neill, "Three-Part Auctions versus Self-Commitment in Day-ahead Electricity Markets," *Utilities Policy*, vol. 18, pp. 165–173, December 2010.
[41] R. Sioshansi and A. Tignor, "Do Centrally Committed Electricity Markets Provide Useful Price Signals?" *The Energy Journal*, vol. 33, pp. 97–118, 2012.
[42] J. King, A. Clifton, and B.-M. Hodge, "Validation of Power Output for the WIND Toolkit," National Renewable Energy Laboratory, Golden, CO, Tech. Rep. NREL/TP-5D00-61714, September 2014.
[43] C. Draxl, B.-M. Hodge, A. Clifton, and J. McCaa, "Overview and Meteorological Validation of the Wind Integration National Dataset Toolkit," National Renewable Energy Laboratory, Golden, CO, Tech. Rep. NREL/TP-5000-61740, April 2015.
[44] C. Draxl, A. Clifton, B.-M. Hodge, and J. McCaa, "The Wind Integration National Dataset (WIND) Toolkit," *Applied Energy*, vol. 151, pp. 353–366, 1 August 2015.

Mahan A. Mansouri holds the B.A. degree in electrical engineering from Azad University of Tehran and the M.Sc. in electrical and computer engineering from The Ohio State University. He is a Ph.D. student in Department of Integrated Systems Engineering at The Ohio State University. His research focuses on renewable-energy and restructured-electricity-market analysis, demand management for ancillary services, load forecasting, generation-fleet optimization, and transmission-business assessment.

Ramteen Sioshansi holds the B.A. degree in economics and applied mathematics and the M.S. and Ph.D. degrees in industrial engineering and operations research from University of California, Berkeley, and an M.Sc. in econometrics and mathematical economics from London School of Economics and Political Science. He is a professor in Department of Integrated Systems Engineering and Department of Electrical and Computer Engineering and an associate fellow in Center for Automotive Research at The Ohio State University, Columbus, OH. His research focuses on renewable and sustainable energy system analysis and the design of restructured competitive electricity markets.